Applied Catalysis B: Environmental 193 (2016) 180–188

Contents lists available at ScienceDirect

Applied Catalysis B: Environmental

journal homepage: www.elsevier.com/locate/apcatb

Ultra-deep desulfurization of gasoline through aqueous phase in-situ hydrogenation and photocatalytic oxidation

Lei Wang[a,*], Wenya Wang[a], Nchare Mominou[c], Luoxin Liu[b], Shuzhen Li[a,*]

[a] Shanghai Institute of Technology, Shanghai 201418, PR China
[b] SINOPEC Luoyang Company, Luoyang 471012, PR China
[c] University of Ngaoundere, Ngaoundere, P.O. BOX 454, 999108, Cameroon

ARTICLE INFO

Article history:
Received 22 August 2015
Received in revised form 21 January 2016
Accepted 15 April 2016
Available online 19 April 2016

Keywords:
Ultra-deep desulfurization
Hydrogenation
Photocatalytic oxidation

ABSTRACT

ZSM-5 zeolite was comodified with zirconium oxide, nickel oxide and titanium oxide. A fixed-bed reactor and a photocatalytic reactor were used to investigate the performance of the resulting catalysts in the desulfurization of fluid catalytic cracking (FCC) gasoline through coupling in-situ hydrogenation with photocatalytic oxidation desulfurization (HPODS). The resultant samples were characterized using the nitrogen adsorption-desorption, X-ray diffraction (XRD) and scanning electron microscope (SEM) techniques. X-ray diffraction analysis indicated the coexistence of ZrO_2, NiO and TiO_2 in the catalysts. The desulfurization rate, the refined oil yield and the increase in the research octane number reached 100%, 99.9% and 2 units, respectively, under suitable conditions of a hydrogenation catalyst weight of 3 g, a catalyst ratio of 1.8, a pressure of 2.0 MPa, a hydrogenation reaction time of 60 min, a hydrogenation temperature of 453 K, an oxidation temperature of 323 K, and an oxidation reaction time of 40 min.

1. Introduction

Ultra-deep desulfurization of fluid catalytic cracking (FCC) gasoline has attracted much attention because of strict government regulations on sulfur discharge considering clean environment and human health. According to these regulations, the upper limit of sulfur content in gasoline is 10 μg/g [1,2].

Hydrodesulfurization (HDS) for the transformation of organic sulfides to sulfur-free organic compounds and hydrogen sulfide represent a valuable and timely technology. However, HDS operates under the conditions of the high temperature, the high pressure and in the presence of hydrogen. Severe conditions make HDS a costly alternative for ultra-deep desulfurization and lead to a decrease in the research octane number of FCC gasoline because of the hydrogenation of aromatic and olefin in the feedstock. Besides, HDS is not effective in the removal of thiophene and its derivatives, especially 4,6-dimethyldibenzothiophene because of its steric hindrance [3–6]. Some important progresses have also been achieved with mild conditions of HDS by applying active catalysts [7].

Owing to the inherent difficulties of HDS for removing thiophenic compounds, many alternative technologies have been studied, for example: biodesulfurization [8,9], selective adsorption [10–13], physical extraction [14–17], oxidative desulfurization (ODS) [18–21], complexation, pervaporation [22–27], and their combinations. Among these desulfurization processes, ODS might be the most feasible route for the desulfurization of FCC gasoline. ODS has received attention because the operating conditions were mild, the desulfurization rate was high, and the research octane number was no loss. Photocatalytic oxidation was regarded as a promising desulfurization process due to the high selectivity and the high desulfurization rate of thiophene and its derivatives. However, according to previous studies [28,29], a certain part of carbons and hydrogens were also removed by oxidants leading to a decrease in refined oil yield when organic sulfides were oxidized to the corresponding sulfoxides and sulfones. Therefore, further increasing the desulfurization rate is still a challenging goal, because a decrease in the refined oil yield and the research octane number is inevitable in the desulfurization of FCC gasoline. However, ODS seems to be more feasible as a subsequent process of HDS because oxidation and hydrogenation are complementary [30]. The hydrogenation activity of the sulfur compounds is thiophenes > BTs > DBTs, while their oxidation activity is just the opposite [31]. Organic sulfides, which was difficult to be removed by HDS, can be easily removed by ODS. Therefore, ultra-deep desulfurization of FCC gasoline would be achieved through the combination of HDS and ODS.

Hydrogen of the liquid phase in-situ hydrogenation is produced from methanol aqueous-phase reforming over catalysts. The production, preservation and transportation of H_2 in the traditional

* Corresponding author.
E-mail address: wllsz119110@sina.com (S. Li).

http://dx.doi.org/10.1016/j.apcatb.2016.04.032
0926-3373/

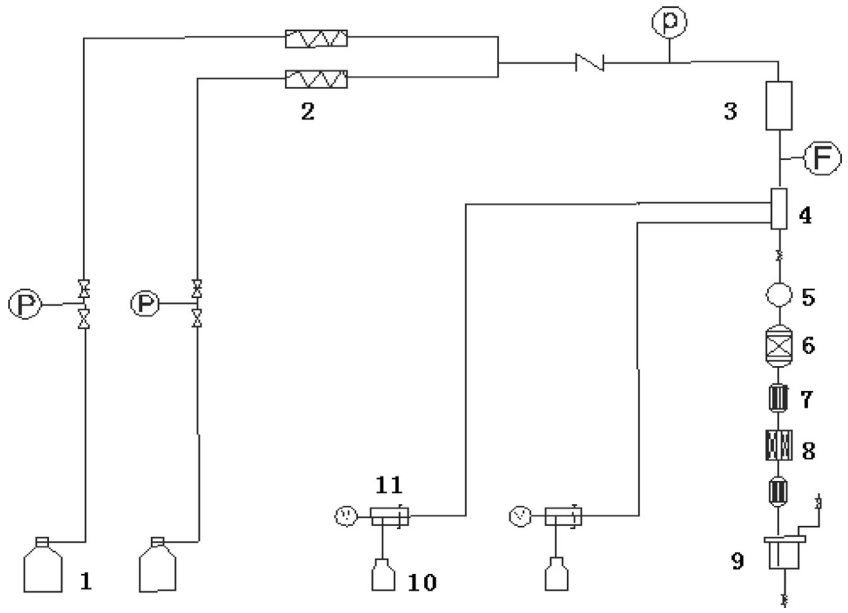

Fig. 1. Schematic diagram of ultra-deep desulfurization of gasoline ((1) air and N_2 cylinders; (2) filters; (3) buffer vessel; (4) mixer; (5) preheater; (6) reactor; (7) cooler; (8) reactor; (9) gas-liquid separator; (10) material tank; (11) bump).

Table 1
Physical properties of FCC gasoline and refined oil.

Items	Properties										
	Distillation range/°C				Octane number		The type of Sulfur content/μg g^{-1}				Total content/μg g^{-1}
	IBP	10%	50%	90%	EP		Thiophene	BT	DBT	Others	
FCC gasoline	48	62	110	182	200	93	478	223	150	349	1200
Refined oil	46	66	116	180	204	95	4	2	0	2	8

hydrogenation process could be eliminated, which leads to the decrease in cost and enhancement of safety significantly. In this process, methanol is the raw material of the aqueous-phase reforming reaction. The active hydrogen generated from the aqueous-phase reforming of methanol could be quickly removed from the active sites of the catalyst, which is superior to the traditional HDS. In this work, ultra-deep desulfurization of FCC gasoline through the aqueous phase in-situ hydrogenation and photocatalytic oxidation desulfurizatoin (HPODS) were investigated with catalysts of ZSM-5 comodified with zirconium, nickel and titanium oxide. This technique could be promising for improving the economic output of refineries.

2. Experimental

2.1. Materials and chemicals

Thiophene, benzothiophene (BT) and dibenzothiophene (DBT) were purchased from Sigma-Aldrich. FCC gasoline (Table 1) was obtained from PetroChina Urumqi Petrochemical Company. Kaolin and zeolite were purchased from Kaolin Co., SINOPEC Catalyst Co., respectively. Pseudo-boehmite powder, diatomite and silica sol were purchased from Shandong Aluminum Industry. Others were bought from the Sinopharm Chemical Reagents Co., Ltd. The model oil was prepared by dissolving thiophene, BT, and DBT in the mixture of *n*-octane, benzene and butylethylene with a sulfur content of 1200 μg/g.

2.2. Preparation and characterization of catalysts

Typical preparation process is described as following.

Seven grams of ZSM zeolite (Si/Al = 180) and 50 mL of deionized water were introduced into a 100 mL flask to form a slurry. The slurry was adjusted with 31 wt% HCl until the pH was 1.5. The mixture was washed with deionized water and filtrated. The filter cake obtained was impregnated with a mixture of hydrochloric acid solution, titanium tetrachloride (5 g), Zirconium oxychloride (2.8 g) and nickel nitrate (3.4 g) at 313 K for 2 h; dried at 403 K for 5 h; and calcined at 673 K for 3 h to obtained ZrO_2/NiO-TiO_2-ZSM-5.

The crystallinity of the catalysts was characterized by X-ray diffraction (XRD; D/Max 2500X; worked at 40 kV and 100 mA, CuKα source). The valence states of active metals of samples were characterized by Fourier Translation Infrared Spectroscopy (FT-IR). The morphology and size were characterized with scanning electron microscopy (SEM; JEOL, JSM-6480A). The pore size and volume distribution were measured with nitrogen adsorption-desorption (Quantarome NOVA 4000) at 77 K. The surface areas of the samples were determined according to the Brunauer-Emmett-Teller (BET) equation. The acidity was characterized by the temperature programmed desorption of ammonia (NH_3-TPD) in a dynamic chemisorption analyzer (Micromeritics ASAP 2920).Pyridine-adsorbed infrared (Py-FTIR) spectra were used to discriminate acid type of samples by EQUINOX 70 (Buker, Germany).

2.3. Desulfurization testing

The desulfurization of gasoline was carried out in a fixed bed reactor and a photocatalytic reactor equipped with mercury lamps (100 w; a main peak 254 nm). A scheme of the reaction setup is shown in Fig. 1. First, ZrO_2/NiO-TiO_2-ZSM-5 in the hydrogenation reactor (3 g) and photocatalytic reactor (1.6 g) was

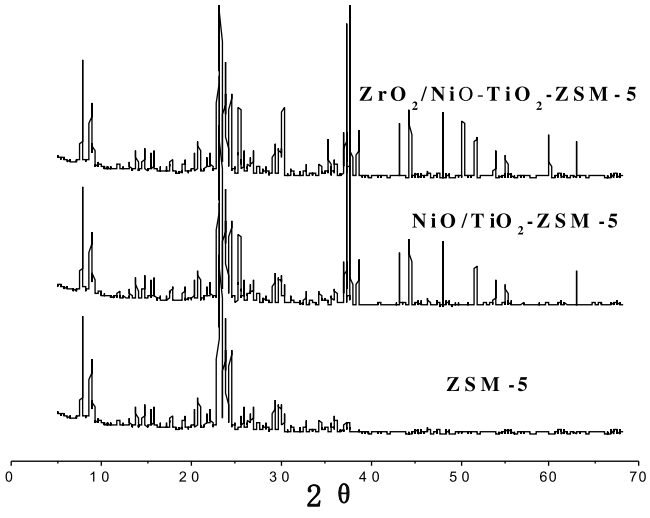

Fig. 2. XRD patterns of catalysts ZSM-5 (Si/Al ratio of 180), ZrO_2/NiO-TiO_2-ZSM-5 (Ni:Zr:Ti = 1.5:1:1, metal content 15%).

activated at 573 K for 1 h under a nitrogen atmosphere. The reactor of in-situ hydrogenation was heated gradually to the reaction temperature, FCC gasoline 1 mL/min and methanol (a hydrogen donor) 0.01 mL/min were preheated to 423 K, and fed into the in-situ hydrogenation reactor. Meanwhile, hydrogen peroxide 0.004 mL/min was preheated to 323 K, and introduced into the photocatalytic oxidation reactor. After the desulfurization, the products were cooled, separated with a gas-liquid separator, and then analyzed by gas chromatography with atomic emission detector.

3. Results and discussion

3.1. Physicochemical properties of catalysts

XRD patterns of ZSM-5 (Si/Al ratio of 180), NiO/TiO_2-ZSM-5 and ZrO_2/NiO-TiO_2-ZSM-5 are presented in Fig. 2. These patterns show distinct sharp diffraction peaks at 5–10° and 20–25° (2θ) in agreement with the typical pattern of the ZSM-5 crystal structure. The XRD patterns of the three catalysts are mainly identical. The basic structure of ZSM-5 is not remarkable consorted and even destroyed since the modification of the catalysts by Zr, Ni and Ti species. Several small diffraction peaks at 2θ values of 30.26°, 35.35°, 50.31°, and 59.93° are assigned to ZrO_2 crystals [PDF#65-6357]. The peaks at 37.23°, 43.26°, 63.01° [PDF#44-1159] and 25.37°, 37.02°, 37.77°, 38.63°, 48.12°, 53.91°, 55.12° [PDF#29-1360] are attributed to NiO and TiO_2 crystals, respectively.

Table 2
The characteristic of catalysts.

Items	ZSM-5	NiO/TiO_2-ZSM-5	ZrO_2/NiO-TiO_2-ZSM-5
Crystallite size (nm)	7.1	7.6	8.2
Pore size of catalyst (nm)	15.6	14.3	13.9
BET surface area (m^2/g)	356	354	349
Micropore area (m^2/g)	215	213	209
Total pore volume (mL/g)	0.36	0.34	0.31
Micropore volume (mL/g)	0.099	0.094	0.092
Desulfurization rate %	75	97	99.0

Table 3
Effects of Si/Al ratios on the desulfurization rate.

Si/Al ratio	Desulfurization rate/%	RON	Strong acid/mmol g^{-1}	Total acid/mmol g^{-1}
60	85.3	92.3	0.17	0.29
100	99.5	93.0	0.15	0.28
180	100	95.0	0.11	0.22
200	99.2	93.8	0.08	0.19
230	99.1	93.2	0.05	0.15

NiO/TiO_2-ZSM-5 exhibits a slightly lower surface area than ZSM-5 (Table 2). ZrO_2/NiO-TiO_2-ZSM-5 shows lower surface areas than those of NiO/TiO_2-ZSM-5. Micropore volumes of NiO/TiO_2-ZSM-5 and ZrO_2/NiO-TiO_2-ZSM-5 are also lower than those of ZSM-5. For the NiO/TiO_2-ZSM-5 and ZrO_2/NiO-TiO_2-ZSM-5 catalysts, because of the agglomeration of metal oxide particles, the specific surface area, total pore volume, and pore size of catalysts were reduced after loading with ZrO_2, NiO and TiO_2 [32].

The SEM images in Fig. 3 show the morphologies of ZSM-5 and ZrO_2/NiO-TiO_2-ZSM-5 catalysts. The external surface of ZrO_2/NiO-TiO_2-ZSM-5 exhibited a finer morphology than ZSM-5 because the Zr, Ni and Ti species were deposited on the surface of ZSM-5. Both ZSM-5 and ZrO_2/NiO-TiO_2-ZSM-5 were of cubic-like shape and approximately 1–10 μm in size.

The NH_3-TPD spectra in Fig. 4 show the peaks at desorption temperature of 423–583 K and 583–773 K represent the weak acid sites and strong acid sites, respectively. The weak acid relative peak area decreases, the strong acid relative peak area gradually increased, and the total acid increased gradually as the ratio of Si/Al was increased. The ratio of strong acid/weak acid was 1:1 when the ratio of Si/Al was 180 (Table 3).

The FT-IR spectra of ZrO_2/NiO-TiO_2-ZSM-5 show the valence states of active metals (Fig. 5). Vibration absorption peaks at

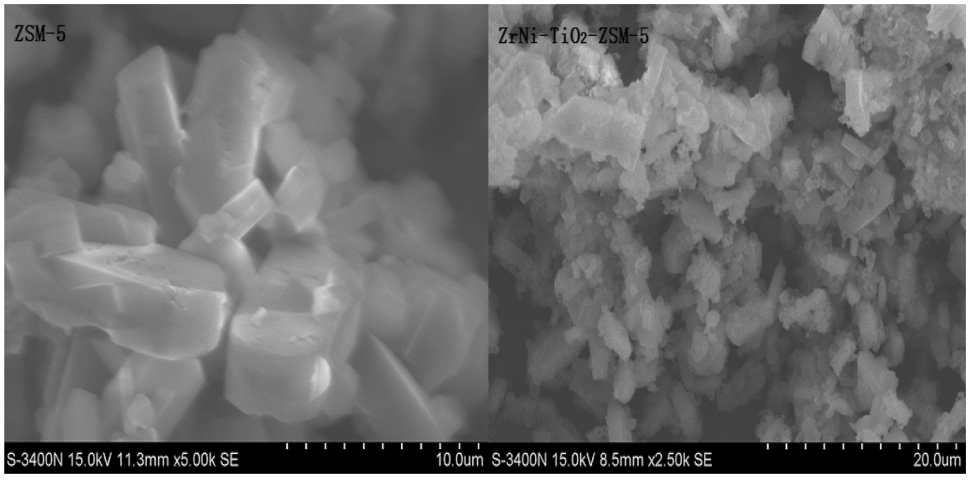

Fig. 3. SEM images of catalysts ZSM-5 (Si/Al ratio of 180), ZrO_2/NiO-TiO_2-ZSM-5 (Ni:Zr:Ti = 1.5:1:1 and 15% metal content).

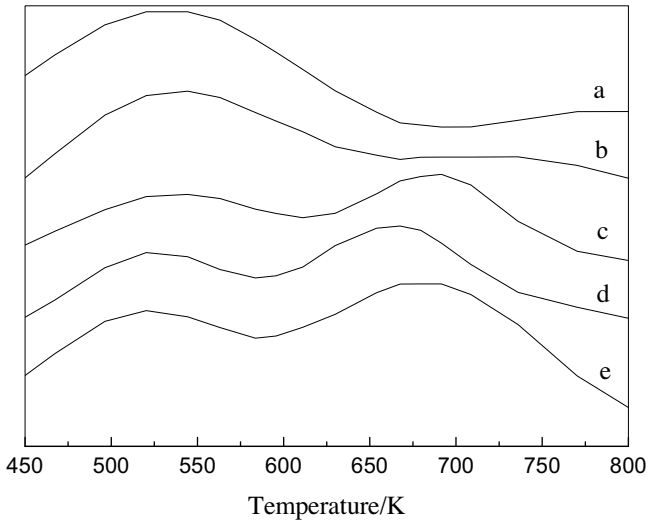

Fig. 4. NH_3-TPD patterns of catalysts with different Si/Al ratios ((a) Si/Al = 230; (b) Si/Al = 200; (c) Si/Al = 180; (d) Si/Al = 100; (e) Si/Al = 60).

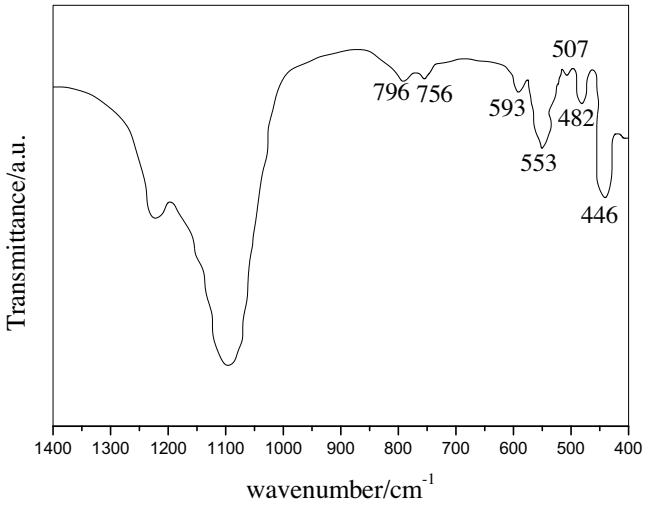

Fig. 5. FT-IR spectra of ZrO_2/NiO-TiO_2-ZSM-5.

Table 4
Acid type of samples.

samples	B acid/mmol g^{-1}	L acid/mmol g^{-1}	B/L
ZSM-5	0.161	0.015	10.67
TiO_2-ZSM-5	0.171	0.020	8.6
NiO/TiO_2-ZSM-5	0.185	0.019	9.5
ZrO_2/NiO-TiO_2-ZSM-5	0.208	0.015	13.9

756 cm^{-1},593 cm^{-1}, and 507 cm^{-1} are assigned to ZrO_2. Peaks at 796 cm^{-1}, 553 cm^{-1}, and 446 cm^{-1} are attributed to TiO_2. The peak at 482 cm^{-1} represents NiO. There are no peaks at 960 cm^{-1} show metal oxides supported on the ZSM-5 in agreement with the results of XRD.

There are three absorption peaks in the range of 1400–1600 cm^{-1} (Fig. 6). The peak at 1490 cm^{-1} represents B acid and L acid. The peaks at 1540 cm^{-1} and 1450 cm^{-1} represent B acid and L acid, respectively. The catalyst acidity of ZrO_2/NiO-TiO_2-ZSM-5 changes more obvious, the intensity of the B acid peak enhanced obviously. An increase in B acid and a decrease in L acid, but the ratio of B/L is 1.3 times as much as ZSM-5 (Table 4).

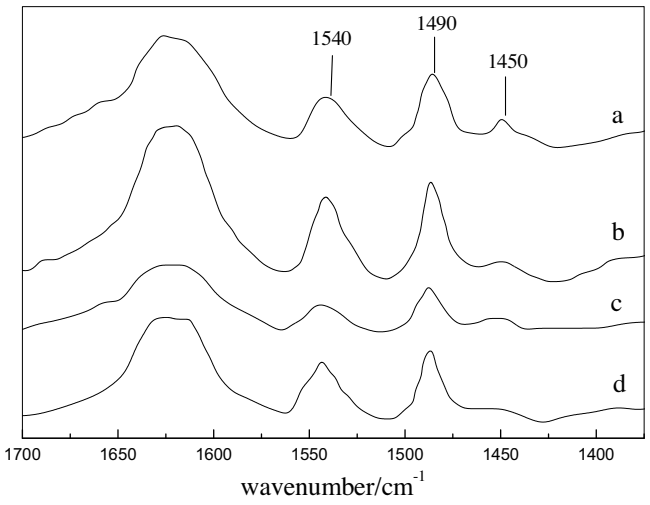

Fig. 6. Py-FTIR spectra of ZSM-5, ZrO_2/NiO-TiO_2-ZSM-5, TiO_2-ZSM-5 and NiO/TiO_2-ZSM-5 ((a) TiO_2-ZSM-5; (b) ZrO_2/NiO-TiO_2-ZSM-5; (c) ZSM-5; (d) NiO/TiO_2-ZSM-5).

Table 5
Comparison of in situ hydrogenation, photocatalyst oxidation and HPODS.

	Items	Model oil	FCC gasoline
Desulfurization rate %	In situ hydrogenation	96.5	94.6
	Photocatalyst oxidation	98.8	95.6
	HPODS	100	100
Refine oil yield %	In situ hydrogenation	99.5	99.6
	Photocatalyst oxidation	98.5	98.9
	HPODS	99.9	99.8

3.2. *Effects of the Si/Al ratio on the desulfurization rate*

The Si/Al ratio of catalyst influences on both the desulfurization rate and the octane number of FCC gasoline.

Samples with different Si/Al ratios (Table 5) indicated that a Si/Al ratio of 180 was a suitable for the desulfurization rate and the octane number of FCC gasoline. The desulfurization rate and the octane number increased, reached a maximum, and then decreased as the Si/Al ratio was increased from 60 to 230. As the ratio of Si/Al increases from 60 to 180, the strong acid sites and the total acid sites were decreased. The strong acid/weak acid ratio of 1 was conducive to the desulfurization reaction and the hydrocarbons transfer reactions such as alkylation, hydroisomerization, aromatization, and little cracking in the HPODS process. Reaction active sites were decreased sharply and resulted in the decrease in the desulfurization rate as the Si/Al ratio was increased further.

3.3. *Influence of metal content on desulfurization rate*

Increasing the content of zirconium, nickel and titanium oxide can improve the catalytic activity of ZrO_2/NiO-TiO_2-ZSM-5 (Si/Al ratio of 180) for the desulfurization rate of FCC gasoline.

Desulfurization rates increase rapidly and reach a peak at the Ni:Ti:Zr weight ratio of 1.5:1:1 (Fig. 7). A gradual increase and a slight decrease of desulfurization rate appear before and after the ratio increases higher than 1.5:1:1, respectively. The highest desulfurization rate of FCC gasoline was reached at a 15% Zr-Ni-Ti content. The desulfurization rate of FCC gasoline increased rapidly to a plateau with a peak of 100% with increasing Zr-Ni-Ti content. The catalyst with 15% (wt%) Zr-Ni-Ti content exhibited the best performance. ZSM-5 showed negligible activity for desulfurization rate, whereas addition of Ni-Zr-Ti species increased the activity. Therefore, the variation of desulfurization rate should be related to metal dispersion on ZSM-5 surface. The decrease in the desulfuriza-

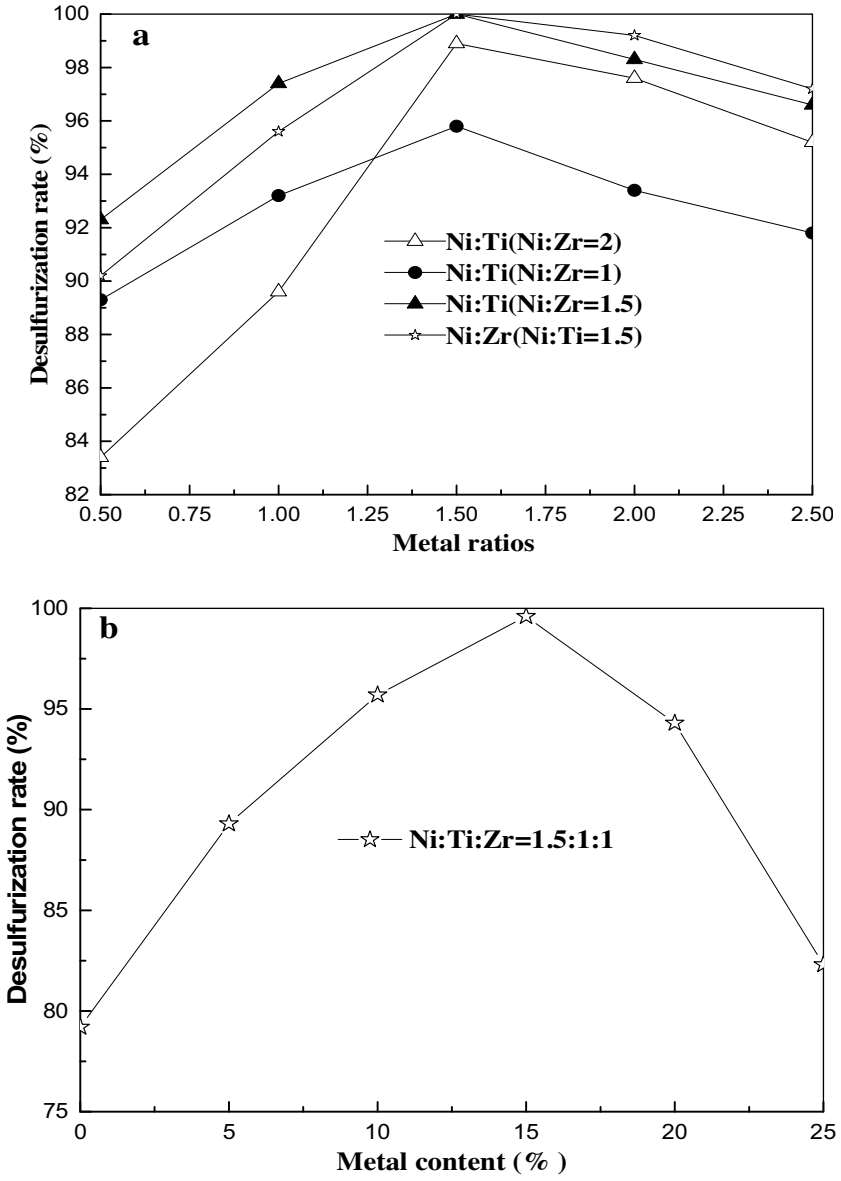

Fig. 7. Influence of the metal content on desulfurization rate.

tion rate at high metal contents can be ascribed to the decreasing accessibility of active sites. Particles in the first layer can be covered by the second layer until large metal oxide agglomerates formed on ZSM-5 surface [33–37]. Owing to the presence of different active sites, ZrO_2/NiO-TiO_2-ZSM-5 is active for the desulfurization of FCC gasoline.

3.4. Different technologies on the desulfurization rate of FCC gasoline

In-situ hydrogenation, photocatalyst oxidation and HPODS exhibited significant differences on the desulfurization rate of model oil and FCC gasoline (Table 5). HPODS was the most favorite for the desulfurization of FCC gasoline. The desulfurization rate of in-situ hydrogenation, photocatalytic oxi and HPODS were 96.5%, 98.8% and 100%, respectively. Refined oil yield of in-situ hydrogenation, photocatalytic oxidation, and HPODS were 99.5%, 98.5% and 99.9%, respectively. The bulky BT and DBT are easier to be oxidized than thiophene because election densities of sulfur atoms in BT and DBT are higher than thiophene. On the contrary, thiophene is easier to be hydrodesulfurized than BT and DBT because of steric effect of the phenyl ring. HPODS exhibited the performance of the ultra-deep removal of thiophene, BT and DBT. When the ultraviolet was absent, a slight decrease in the desulfurization rate (98.5%) was observed for the desulfurization of FCC gasoline.

3.5. Effect of catalyst weight on desulfurization rate of FCC gasoline

The effects of weight ratios (hydrogenation/photocatalytic oxidation) and hydrogenation catalyst weight on the desulfurization rate and the refined oil yield for FCC gasoline were investigated under the optimal conditions.

The desulfurization rate increases from 94.2 to 100%, and the refined oil yield increases from 95.3 to 99.3% when the ratio increases from 0.2 to 1.8 (Fig. 8). With a further increase in the ratio, desulfurization rate and the refined oil yield decrease progressively. Usually, the active site number for the desulfurization is a function of catalytic weight. Desulfurization rate increases with increasing active sites. However, excessive amounts of catalyst were of no

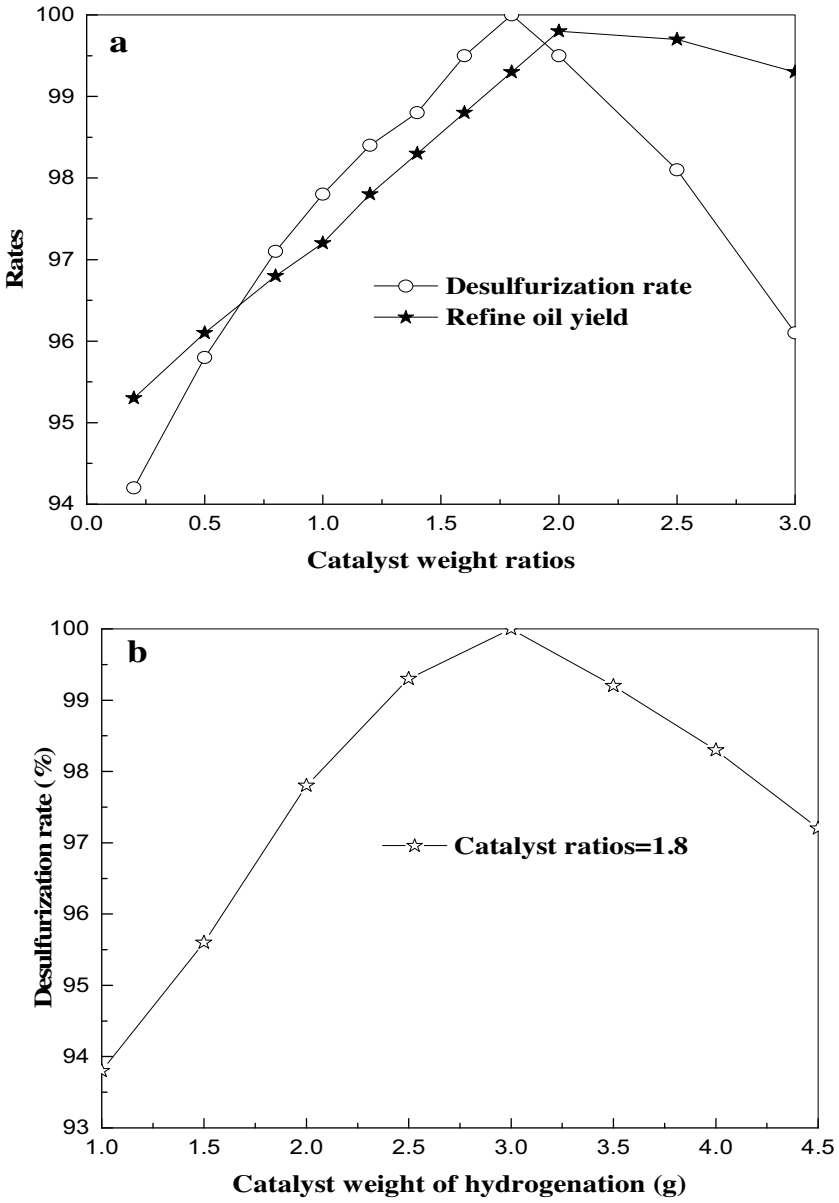

Fig. 8. Effect of catalytic weight on desulfurization rate.

worth for effective sites. Only at a suitable catalyst weight could good catalytic selectivity be obtained and maintained during the reaction process. Therefore, hydrogenation catalyst weight of 3 g and the catalyst ratio of 1.8:1 are more appropriate.

3.6. *Effect of temperature on desulfurization rate of FCC gasoline*

Temperature effect on desulfurization rate of FCC gasoline was also investigated with ZrO_2/NiO-TiO_2-ZSM-5 (Si/Al ratio of 180, Ni:Ti: Zr ratio of 1.5:1:1, metal content of 15%) at a pressure of 2.0 MPa, a reaction time of 30 min, a hydrogenation catalytic weight of 3 g and a catalyst ratio of 1.8:1.

When the hydrogenation temperature was increased from 373 to 513 K, the desulfurization rate gradually increased, reached a maximum (100%), and then gradually decreased as the temperature was increased further (Fig. 9). Temperature has a promotion on hydrogenation and aqueous phase reforming of methanol. Therefore, the increase in temperature has an advantage not only to the reforming of methanol but also to the hydrogenation. For the in-situ hydrogenation of sulfides, the desulfurization rate reached a maximum at 453 K. Increasing the temperature is in favor of hydrogenation reaction of sulfides, But the desulfurization rate decreased at a higher temperature, which might be because the selectivity of hydrogen decreased in the aqueous phase reforming of methanol with increasing the temperature [38].

The desulfurization rate gradually increased from 83.6 to 100% when the photocatalytic oxidation temperature was increased from 293 to 323 K. The desulfurization rate gradually decreased as the temperature increased further. The lower selectivity might be due to the fast decomposition of hydrogen peroxide when the reaction temperature was higher than 323 K.

The desulfurization rate increased rapidly to a plateau with a peak of 99.9% with increasing in-situ hydrogenation pressure (Fig. 10), and then decreased progressively as the pressure was increased further. This might be because the in-situ hydrogenation reaction was the consecutive reaction with the aqueous phase

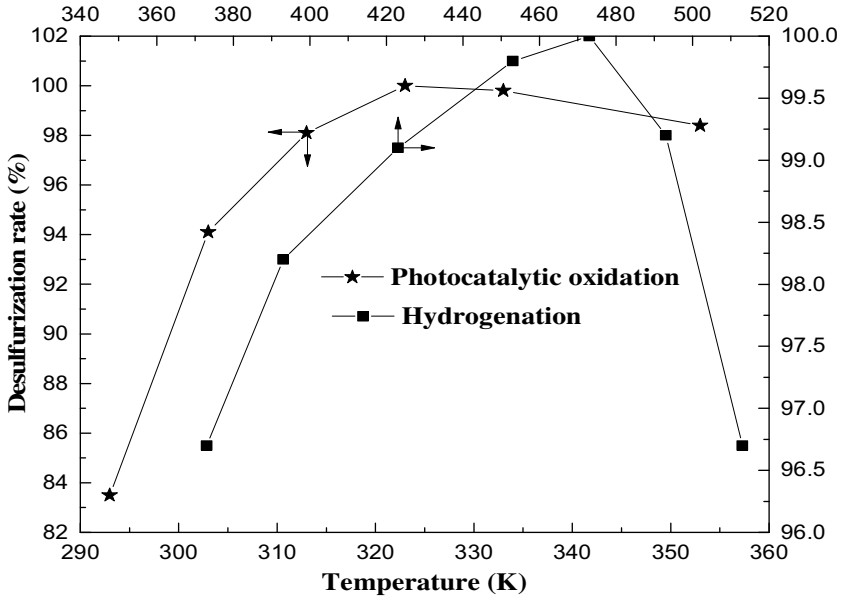

Fig. 9. Effect of temperature on the desulfurization rate by HPODS.

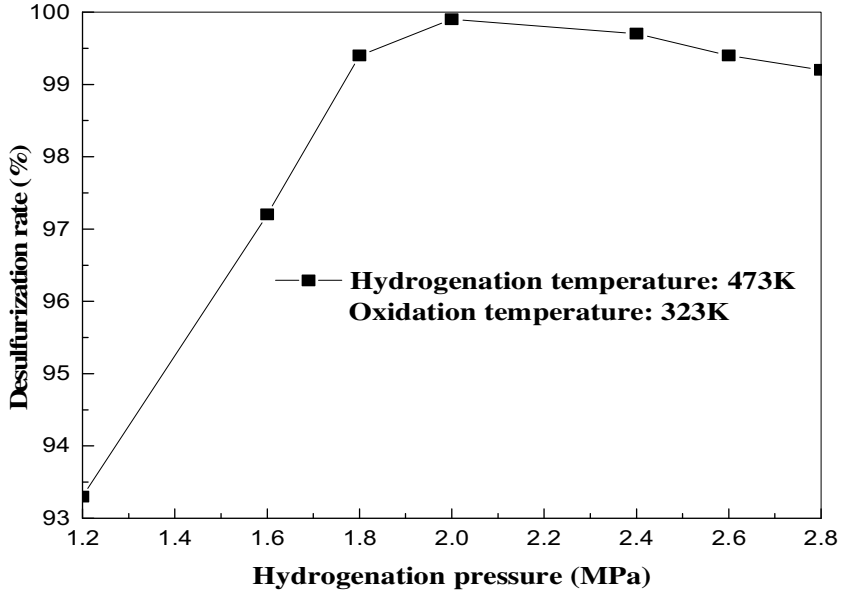

Fig. 10. Effect of pressure on the desulfurization rate by HPODS.

reforming of methanol. The consumption of hydrogen in the in-situ hydrogen desulfurization promoted the hydrogen production and improved the selectivity of hydrogen.

3.7. Effect of reaction time on desulfurization rate of FCC gasoline

The desulfurization rate is determined by the number of reactant molecules on the inner surface of ZrO_2/NiO-TiO_2-ZSM-5. Therefore, it is important to control the reaction time.

A consistent increase in desulfurization rate was observed with increasing reaction time (Fig. 11). When the hydrogenation time and oxidation time was 60 min and 40 min, respectively, the desulfurization rate reached a maximum of 100%. The hydrogenation time of 60 min and oxidation time of 40 min was favorable for the desulfurization of FCC gasoline.

It is well-known that more effective electrons congregated on the sulfur atom contribute to oxidation. The sulfur atom of thiophene has the electron density of 5.596, which is not enough to be oxidized by H_2O_2 as reported by Otsuki [39]. The electron densities of BT and DBT were 5.739 and 5.858, respectively, which can be more easily oxidized into the corresponding sulfones or sulfoxides. Therefore, the reactivity of sulfur removal increased in the order TH < BT < DBT, which may be related to the electron density of the S atom and steric hindrance of the substituent on the substrates [40].

3.8. Effect of the oxidant dosage on desulfurization rate of FCC gasoline

Different oxidant (H_2O_2) dosages were investigated in desulfurization of FCC gasoline with ZrO_2/NiO-TiO_2-ZSM-5 catalysts at a pressure of 2.0 MPa, a reaction time of 30 min, a hydrogenation catalytic weight of 3 g and a catalyst ratio of 1.8.

Desulfurization rate significantly increased as oxidant dosages were increased from 0.1 to 0.4% (Fig. 12), reached a maximum of

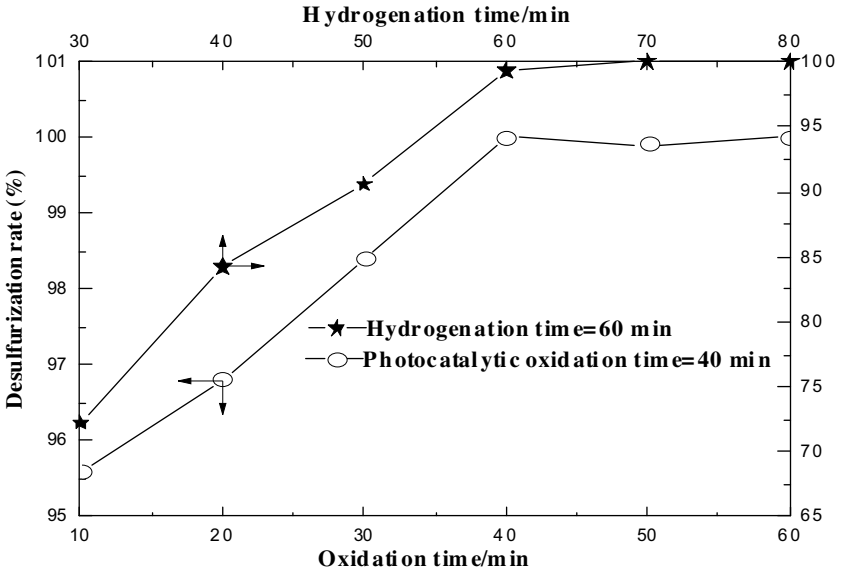

Fig. 11. Effect of reaction time on the desulfurization rate.

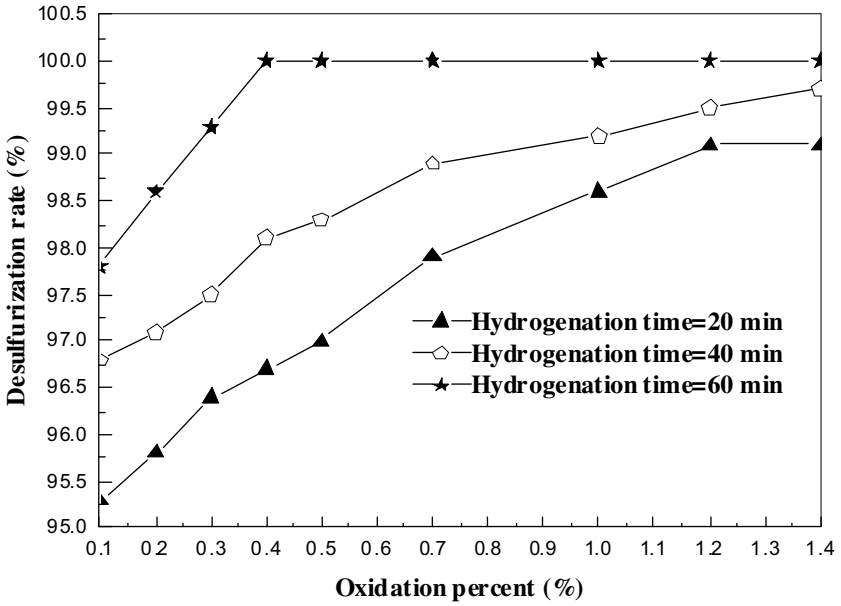

Fig. 12. Effect of the oxidant dosage on the desulfurization rate.

100% at the oxidant dosage of 0.4%, and then slightly decreased with a further increase in oxidant dosage. This trend in desulfurization rate is consistent with the results of refs [41,42], and indicates the balance between two opposite causes: the excess of oxidants increase the desulfurization rate, whereas, the water produced in the oxidation desulfurization reaction and thermal decomposition of oxidants hindered the reaction. Meanwhile, the research octane number of FCC gasoline (unrefined) and refined oil were 93 and 95, respectively. The contents of iso-paraffins and aromatics were increased while the content of olefins of refined oil was decreased (Table 6). The research octane number is related to the composition of gasoline. For hydrocarbons with the same number of carbon atoms and the same molecular weight, the research octane number of hydrocarbons is increased by the following: aromatic hydrocarbons, isoparaffins > naphthenic hydrocarbons, olefins > normal paraffins. We assumed that the increase in the research octane number of FCC gasoline was due to the hydrocarbons transfer reactions such as alkylation, aromatization, and little cracking in the HPODS process. The mechanism needs to be further studied. It is useful to point out that both a higher oxidant dosage and a longer hydrogenation time are necessary to reach the desulfurization rate of 100%. A possible explanation might be that peroxide produced O^{2-} species on the ZrO_2/NiO-TiO_2-ZSM-5 under the condition of ultraviolet irradiating, which lessened the e^-/h^+ recombination rate.

Table 6
The distribution of products of refined oil and FCC gasoline.

Materials	Paraffins/iso-paraffins/v%	Olefins/v%	Aromatics/v%
FCC gasoline	45.2/28.3	36.4	18.4
Refined oil	48.2/32.3	33.0	18.8

Meanwhile, there was a competition between the sulfur compound oxidation and the decomposition of oxidants. The increase

in H_2O_2 dosage could produce more hydroxyl radicals, which were helpful to the oxidation desulfurization. On the other hand, more H_2O_2 dosages also speeded up decomposition which affected unfavorably on the oxidation reaction. Only at a suitable oxidant dosage of 0.4%, could good catalytic selectivity be obtained and maintained during the reaction process.

3.9. Recycling and stability of catalyst

Re-usability of ZrO_2/NiO-TiO_2-ZSM-5 catalysts for desulfurization of FCC gasoline was also investigated. The desulfurization rate preserved 100% for the second time, and decreased to 95.8% for the sixth time because of the instability of the catalysts. Therefore, ZrO_2/NiO-TiO_2-ZSM-5 could be applied as a long-life catalyst for HPODS.

4. Conclusions

In conclusion, ZSM-5 was modified with different elements (Zr, Ni and Ti) for use in ultra-deep desulfurization of FCC gasoline. The results of the study of the catalysts indicated that the presence of Zr, Ni and Ti species in ZSM-5 enhanced the activity for the desulfurization of FCC gasoline through HPODS. The desulfurization rate and refined oil yield reached 100% and 99.9%, respectively, Sulfur compound content of FCC gasoline was reduced from 1200 to 8 μg/g, and the research octane number was increased by 2 units at the suitable conditions.

References

[1] L. Wang, Y.N. Zhang, Y.L. Zhang, P. Liu, H.X. Han, M. Yang, et al., Hydrodesulfurization of 4,6-DMDBT on a multi-metallic sulfide catalyst with layered structure, Appl. Catal. A Gen. 394 (2011) 18–24.
[2] H.W. Zheng, Z.H. Sun, X.L. Chen, Q. Zhao, X.H. Wang, Z.J. Jiang, A micro reaction-controlled phase-transfer catalyst for oxidative desulfurization based on polyoxometalate modified silica, Appl. Catal. A Gen. 467 (2013) 26–32.
[3] K.H. Choi, Y. Korai, I. Mochida, J.W. Ryu, W. Min, Impact of removal extent of nitrogen species in gas oil on its HDS performance: an efficient approach to its ultra deep desulfurization, Appl. Catal. B Environ. 50 (2004) 9–16.
[4] T.A. Zepeda, B. Pawelec, J. León, J. Reyes, A. Olivas, Effect of gallium loading on the hydrodesulfurization activity of unsupported Ga_2S_3/WS_2 catalysts, Appl. Catal. B: Environ. 112 (2012) 10–19.
[5] B. Pawelec, R. Mariscal, R.M. Navarro, M.J. Campos-Martin, J.L.G. Fierro, Simultaneous 1-pentene hydroisomerisation and thiophene hydrodesulphurisation over sulphided Ni/FAU and Ni/ZSM-5 catalysts, Appl. Catal. A Gen. 262 (2004) 155–166.
[6] T.A. Zepeda, A. Infantes-Molina, J.N. Díaz de León, S. Fuentes, G. Alonso-Núnez, G. Torres-Otanez, et al., Hydrodesulfurization enhancement of heavy and light S-hydrocarbons on NiMo/HMS catalysts modified with Al and P, Appl. Catal. A Gen. 484 (2004) 108–121.
[7] H.Y. Song, J.J. Gao, X.Y. Chen, J. He, C.H.X. Li, Catalytic oxidation-extractive desulfurization for model oil using inorganic oxysalts as oxidant and Lewis acid-organic acid mixture as catalyst and extractant, Appl. Catal. A Gen. 456 (2013) 67–74.
[8] S.H.H. Zhang, H. Chen, W. Li, Kinetic analysis of biodesulfurization of model oil containing multiple alkyl dibenzothiophenes, Appl. Microbiol. Biotechnol. 97 (2013) 2193–2200.
[9] V. Chandra Srivastava, An evaluation of desulfurization technologies for sulfur removal from liquid fuels, RSC Adv. 2 (2012) 759–783.
[10] S. Kumar, V. Chandra Srivastava, R.P. Badoni, Studies on adsorptive desulfurization by zirconia based adsorbents, Fuel 90 (2011) 3209–3216.
[11] J.H. Kim, X.L. Ma, A.N. Zhou, C.S. Song, Ultra-deep desulfurization and denitrogenation of diesel fuel by selective adsorption over three different adsorbents: a study on adsorptive selectivity and mechanism, Catal. Today 111 (2006) 74–83.
[12] Y. Shen, P. Li, X. Xu, H. Liu, Selective adsorption for removing sulfur: a potential ultra-deep desulfurization approach of jet fuels, RSC Adv. 2 (2012) 1700–1711.
[13] X. Ma, S. Velu, J.H. Kim, C. Song, Deep desulfurization of gasoline by selective adsorption over solid adsorbents and impact of analytical methods on ppm level sulfur quantification for fuel cell applications, Appl. Catal. B Environ. 56 (2005) 137–147.
[14] X.J. Yu, H.L. Hao, J. Zhang, G. Zheng, B.H. Yao, Desulfurization of fuel oils by extraction with ionic liquids, Adv. Mater. Res. 398 (2012) 2221–2224.
[15] L. Kuznetsova, L.G. Detusheva, N.I. Kuznetsov, V.K. Duplyakin, V.A. Likholobov, Liquid-phase oxidation of benzothiophene and dibenzothiophene by cumyl hydroperoxide in the presence of catalysts based on supported metal oxides, Kinet. Catal. 49 (2008) 644–652.
[16] G. Yu, X. Li, X. Liu, C. Asumana, X. Chen, Deep desulfurization of fuel oils using low-viscosity 1-ethyl-3-methylimidazolium dicyanamide ionic liquid, Ind. Eng. Chem. Res. 50 (2011) 2236–2244.
[17] D. Liu, J. Gui, L. Song, X. Zhang, Z. Sun, Deep desulfurization of diesel fuel by extraction with task-specific ionic liquids, Pet. Sci. Technol. 26 (2008) 973–982.
[18] A.H.M. Shahadat Hussain, B.J. Tatarchuk, Mechanism of hydrocarbon fuel desulfurization using Ag/TiO_2–Al_2O_3 adsorbent, Fuel Process. Technol. 126 (2014) 233–242.
[19] L. Wang, Y.J. Chen, L.C. Du, S.Z. Li, H.J. Cai, W.M. Liu, Nickel-heteropoly acids supported on silica gel for ultra-deep desulfurization assisted by Ultrasound and Ultraviolet, Fuel 105 (2013) 353–357.
[20] X. Si, S. Cheng, Y. Lu, G. Gao, M.Y. He, Oxidative desulfurization of model oil over Au-Ti-MWW, Catal. Lett. 122 (2008) 321–324.
[21] S.F. Cheng, Y.M. Liu, J.B. Gao, L.L. Wang, X.L. Liu, G.H. Gao, et al., Catalytic oxidation of benzothiophene and dibenzothiophene in model light oil over Ti-MWW, Chinese, J. Catal. 27 (2006) 547–549.
[22] J.Q. Huang, J.D. Li, J. Chen, X. Zhan, C.X. Chen, Pervaporation separation of *n*-heptane/organosulfur mixtures with PDMS membrane: experimental and modeling, Can. J. Chem. Eng. 87 (2009) 547–553.
[23] X.L. Fang, W. Wei, Y. Chen, W. Jin, N. Xu, Optimisation of preparation conditions for polydimethylsiloxane (PDMS)/ceramic composite pervaporation membranes using response surface methodology, J. Membr. Sci. 311 (2008) 23–33.
[24] B. Li, S.N. Yu, Z.Y. Jiang, W.P. Liu, R.J. Cao, H. Wu, Efficient desulfurization by polymer organic nanocomposite membranes fabricated in reverse microemulsion, J. Hazard. Mater. 12 (2012) 296–303.
[25] C.W. Zhao, J.D. Li, R.B. Qi, J. Chen, Z.K. Luan, Pervaporation separation of *n*-heptane/sulfur species mixtures with polydimethylsiloxane membranes, Sep. Purif. Techol. 63 (2008) 220–225.
[26] D. Mitra, Desulfurization of gasoline by pervaporation, Sep. Purif. Rev. 41 (2012) 97–125.
[27] R. Cao, X. Zhang, H. Wu, J. Wang, X. Liu, Z. Jiang, Enhanced pervaporative desulfurization by polydimethylsiloxane membranes embedded with silver/silica core-shell microspheres, J. Hazard. Mater. 187 (2011) 324–332.
[28] L. Wang, S.Z. Li, H.J. Cai, Y.Y. Xu, X.H. Wu, Y.J. Chen, Ultra-deep desulfurization of fuel with metal complex of Chitosan Schiff Base assisted by ultraviolet, Fuel 94 (2012) 165–169.
[29] L. Wang, H.J. Cai, S.Z. Li, N. Mominou, Ultra-deep removal of thiophene compounds in diesel oil over catalyst TiO_2/Ni-ZSM-5 assisted by ultraviolet irradiating, Fuel 105 (2013) 752–756.
[30] C.S. Song, X.L. Ma, New design approaches to ultra-clean diesel fuels by deep desulfurization and deep dearomatization, Appl. Catal. B Environ. 41 (2013) 207–238.
[31] R. Javadli, A.D. Klerk, Desulfurization of heavy oil–oxidative desulfurization (ODS) as potential upgrading pathway for oil sands derived bitumen, Energy Fuels 26 (2011) 594–602.
[32] M.A. Al-Daous, S.A. Ali, Deep desulfurization of gas oil over NiMo catalysts supported on alumina-zirconia composites, Fuel 97 (2012) 662–669.
[33] X. Ma, M. Sprague, C. Song, Deep desulfurization of gasoline by selective adsorption over nickel-based adsorbent for fuel cell applications, Ind. Eng. Chem. Res. 44 (2005) 5768–5775.
[34] M.V. Landau, M. Herskowitz, R. Agnihotri, J.E. Kegerreis, Ultra deep adsorption desulfurization of gasoline with Ni/Al-SiO_2 material catalytically facilitated by ethanol, Ind. Eng. Chem. Res. 47 (2008) 6904–6916.
[35] S.L. Lakhapatri, M.A. Abraham, Deactivation due to sulfur poisoning and carbon deposition on Rh-Ni/Al_2O_3 catalyst during steam reforming of sulfur-doped *n*-hexadecane, Appl. Catal. A Gen. 364 (2009) 113–121.
[36] A. Mansouri, A.A. Khodadadi, Y. Mortazavi, Ultra-deep adsorptive desulfurization of a model diesel fuel on regenerable Ni-Cu/γ-Al_2O_3 at low temperatures in absence of hydrogen, J. Hazard. Mater. 271 (2014) 120–130.
[37] S. Otsuki, T. Nonaka, N. Takashima, W.H. Qian, A. Ishihara, T. Imai, et al., Oxidative desulfurization of light gas oil and vacuum gas oil by oxidation and solvent extraction, Energy Fuel 14 (2000) 1232–1239.
[38] Y. Xu, J.X. Long, Q.Y. Liu, Y.B. Li, C.G. Wang, Q. Zhang, et al., In situ hydrogenation of model compounds and raw bio-oil over Raney Ni catalyst, Energy Conv. Manag. 89 (2015) 188–196.
[39] X.T. Wang, W. Chen, Y.F. Song, Directional self-assembly of exfoliated layered europium hydroxide nanosheets and $Na_9EuW_{10}O_{36}\cdot 32H_2O$ for application in desulfurization, Eur. J. Inorg. Chem. 17 (2014) 2779–2786.
[40] S. Kaniou, K. Pitarakis, I. Barlagianni, I. Poulios, Photocatalytic oxidation of sulfamethazine, Chemosphere 60 (2005) 372–380.
[41] G.Q. Luo, L.H. Kang, M.Y. Zhu, B. Dai, Highly active phosphotungstic acid immobilized on amino functionalized MCM-41 for the oxidesulfurization of dibenzothiophene, Fuel Process. Technol. 118 (2014) 20–27.
[42] P. Na, B.L. Zhao, L.Y. Gu, J. Liu, J.Y. Na, Deep desulfurization of model gasoline over photo-irradiated titanium-pillared montmorillonite, J. Phys. Chem. Solids 70 (2009) 1465–1470.